Supporting Information:

Atomic structure and handedness of the building block of a biological assembly

Antoine Loquet, Birgit Habenstein, Veniamin Chevelkov, Suresh Kumar Vasa, Karin Giller, Stefan Becker, Adam Lange*

Max Planck Institute for Biophysical Chemistry, Department of NMR-based Structural Biology, Am Fassberg 11, 37077 Göttingen, Germany

T3SS needle sample preparation

PrgI needles were prepared as reported in ref[1], using [1-^{13}C]glucose, [2-^{13}C]glucose, [1,3-^{13}C]glycerol and [2-^{13}C]glycerol carbon sources. Samples were filled into 4 mm ssNMR rotors.

Solid-state NMR spectroscopy

Experiments were conducted on 14.1 and 20.0 Tesla solid-state NMR spectrometers (BrukerBiospin, Germany), at an MAS rate of 11 kHz. The sample temperature was ~5°C for all experiments. NMR chemical shifts were calibrated using DSS as an internal reference. All 1D cross-polarization spectra (recorded at 20.0 Tesla) shown in Figure SI1-3 were obtained with 160 scans and an acquisition time of 30 ms, using high-power (83 kHz) SPINAL-64[21]^{1}H-^{13}C decoupling during acquisition. A 2D ^{13}C-^{13}C PDSD spectrum (recorded at 14.1 Tesla, mixing time: 850 ms) of [2-^{13}C]glycerol-labeled T3SS needles was recorded with acquisition times of 20 and 15 ms for direct and indirect dimensions, for a total experimental time of 5.3 days. A 2D ^{13}C-^{13}C PDSD spectrum (20.0 Tesla, mixing time: 800 ms) of [2-^{13}C]glycerol-labeled T3SS needles was recorded with acquisition times of 20 and 15 ms for direct and indirect dimensions, for a total experimental time of 4.4 days. A 2D ^{13}C-^{13}C PDSD spectrum (20.0 Tesla, mixing time: 850 ms) of [1,3-^{13}C]glycerol-labeled T3SS needles was recorded with acquisition times of 20 and 18 ms for direct and indirect dimensions, for a total experimental time of 7.5 days. A 3D ^{15}N-^{13}C-^{13}C NCα-PDSD spectrum[3-5] (20.0 Tesla, PDSD mixing time: 850 ms) of [2-^{13}C]glycerol-labeled T3SS needles was recorded with acquisition times of 7, 7 and 20 ms, for a total experimental time of 10.8 days. All NMR spectra were analyzed using CcpNmr[6]. Experimental details about the 2D spectra recorded on selectively glucose-labeled samples were already reported in ref[1].

Structure calculations

ssNMR cross-peaks that encode for long-range interactions were used as internuclear distance restraints with a distance range of 2-8.5Å. CNS (version 1.21[7]) routines were used to perform standard structure calculations. In brief, PrgI monomeric conformers were generated on the basis of intra-subunit restraints and TALOS+[8] dihedral restraints. ^{1}H (Chevelkov et al., submitted), ^{13}C and ^{15}N chemical shifts were used as input for TALOS+ predictions.^{1}H, ^{13}C and ^{15}N chemical shift values are accessible under the BMRB entry 18276.The 10 lowest-energy monomers are shown in Figure SI7A.Inter-subunit restraints were classified into two sets: the axial one (encoding for the (i)-(i+11) interface) and the lateral one (encoding for the (i)-(i+5/6) interfaces). According to the secondary structure topology determined by ssNMR chemical shifts, axial restraints could be unambiguously distinguished (see Figure SI8)[1]. A second round of calculations was used to generate homotrimerPrgI conformers (i.e. trimers of subunits (i), (i+5) and (i+6)). Lateral inter-subunit restraints were introduced with the i+5/6 ambiguity during this calculation round, and we iteratively removed the most violated contributions (violation > 10Å) to solve the i+5/6 ambiguity after each iteration. A total of 6 iterations were used. 640 conformers were calculated at each iteration, and the

100 lowest-energy conformers were used for the violation analysis. This approach is in principle similar to protocols used in automatic software such as ARIA[9] or UNIO[10]. In a final round of calculations, PrgIhomotetramer conformers were generated by adding the axial restraints to the previous input data. A number of 400 conformers were generated for this round of calculation. A bundle of the 15 lowest-energy tetramers (see structural statistics in Table SI1) out of 60 conformers with few restraint violations was used to generate Figure 2. For all structure calculations involving homo-multimers, a noncrystallographic symmetry energy term was used to enforce that different monomers stay superimposable, in order to reproduce the presence of a single subunit conformation[1]. The axial rise per subunit was computed using the bundle of 60 conformers (between subunits i+5 and i+6).

STEM analysis

STEM (scanning transmission electron microscopy) measurements were carried out at Brookhaven National Laboratory (USA). The experimental setup and sample conditions were similar to those described previously[11,12]. Mass calibration was achieved by means of tobacco mosaic virus (TMV) particles, calibrated to 13.1 kDa/Å. The analysis of the images was done using the PCmass software.

A dark-field STEM image of PrgI needles is shown in Fig. 3A. Uniform and well separated individual needles can be observed. The needle segments are fitted with a "9 nm solid rod" model with a length of 30 nm and the model fits very well with individual needles. A few segments and the integrated MPL values are shown. The MPL histogram (Fig. 3B) is fitted with a single Gaussian distribution function and the determined MPL value for the PrgI needle is 2.13 kDa/Å. This corresponds to an axial rise of ~4.25 Å per subunit. From the intermolecular lateraltranslation of ~24 Å, this yields~5.65 subunits per turn. This value matches well with our T3SS needle model for which 11 subunits are packed in two turns (~2×5.5).

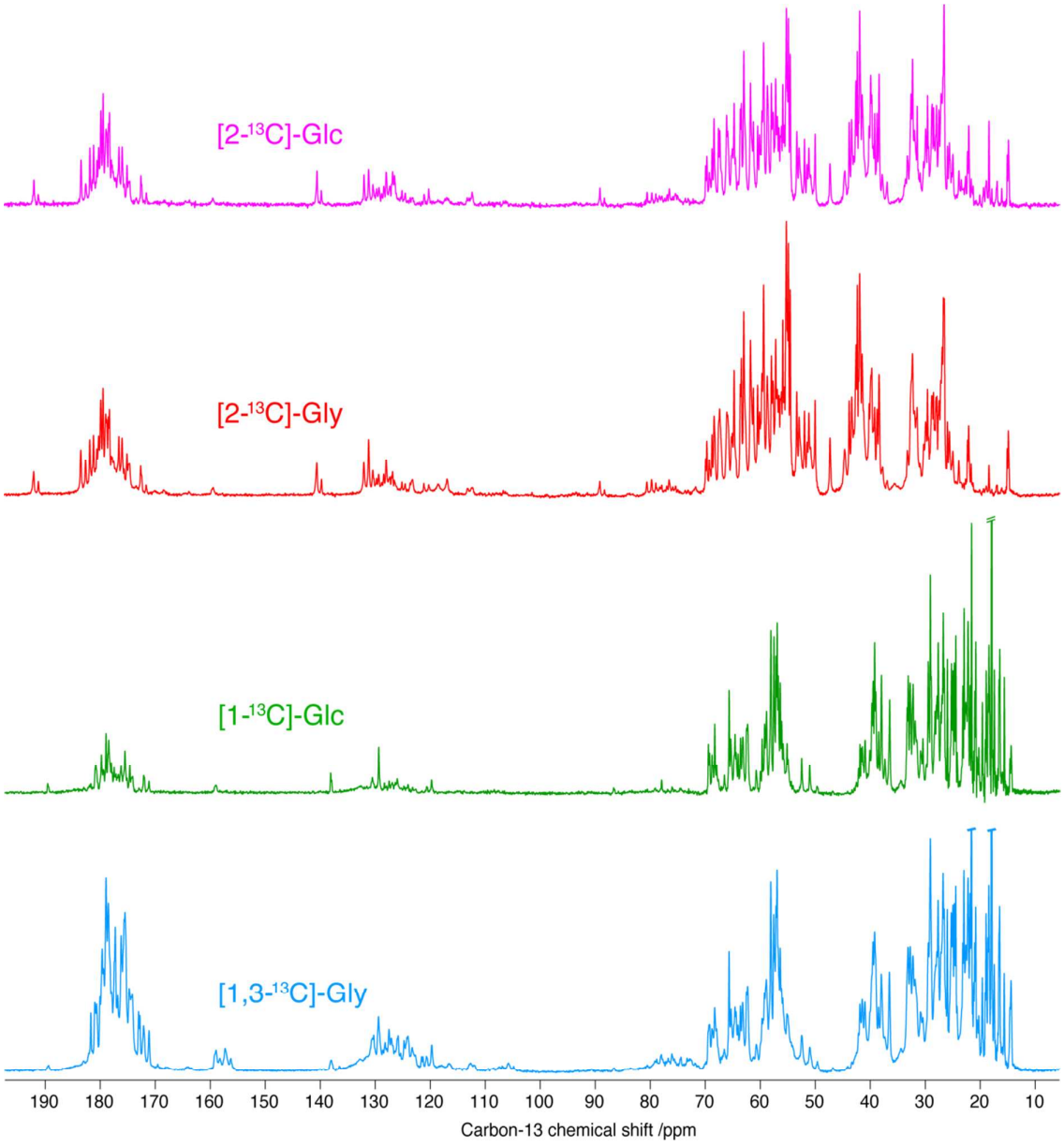

Figure SI1. 1D cross-polarization spectra of the type III secretion system needle labeled with [1-^{13}C]glucose, [2-^{13}C]glucose, [1,3-^{13}C]glycerol and [2-^{13}C]glycerol,respectively.

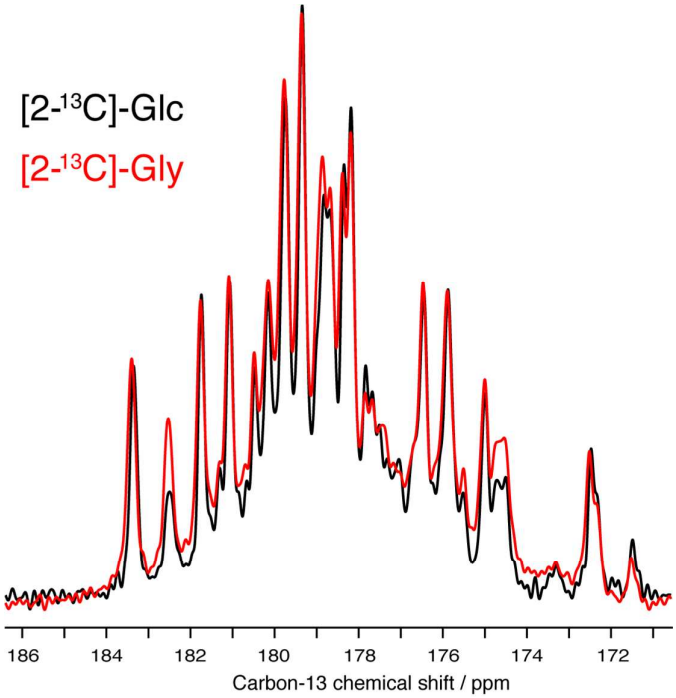

Figure SI2. 1D cross-polarization spectra of the T3SS needle labeled with [2-^{13}C]glucose (in black) and [2-^{13}C]glycerol (in red).

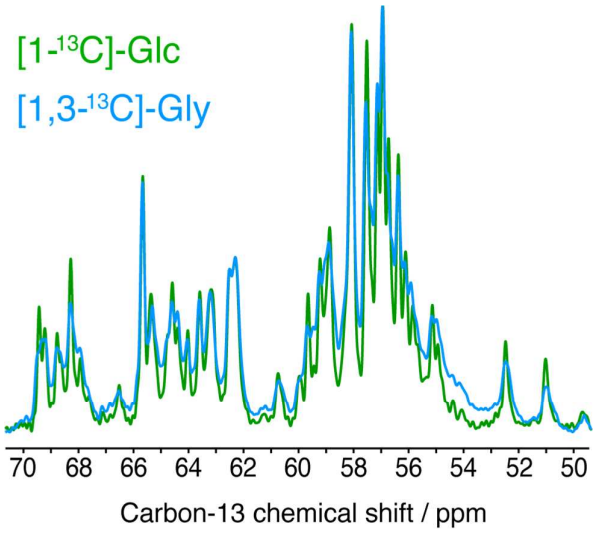

Figure SI3. 1D cross-polarization spectra of the T3SS needle labeled with [1-^{13}C]glucose (in green) and [1,3-^{13}C]glycerol (in blue).

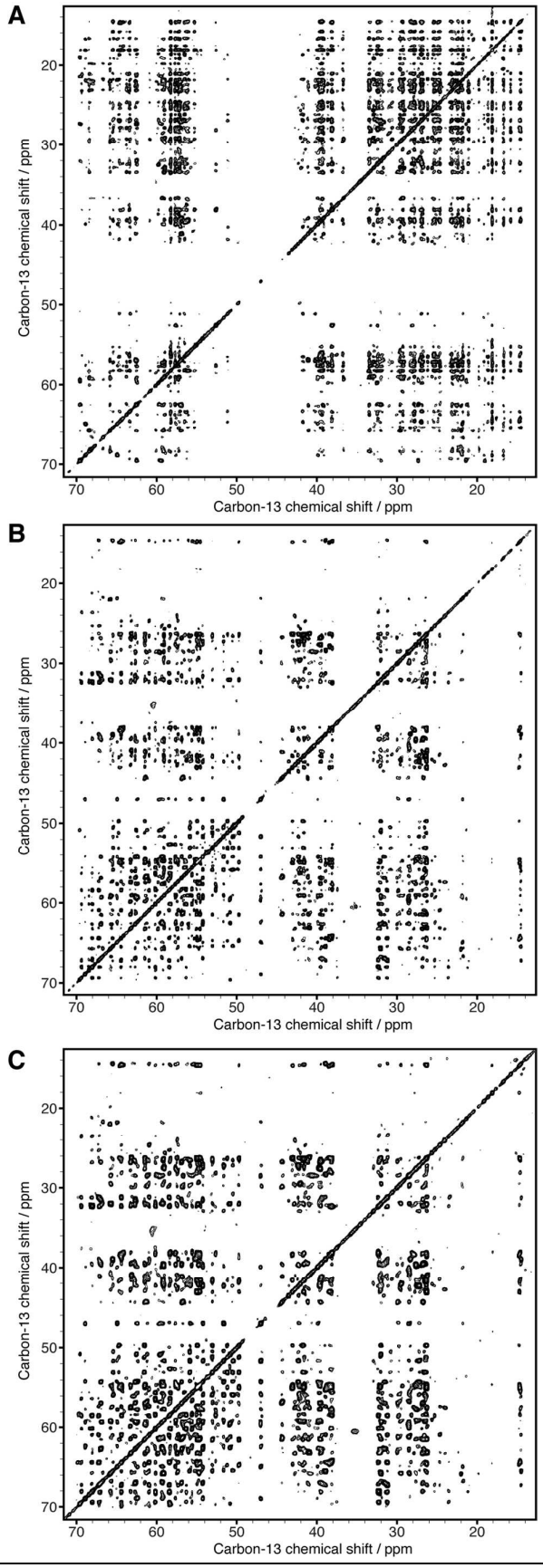
A
B
C
Carbon-13 chemical shift / ppm
Carbon-13 chemical shift / ppm
20
30
40
50
60
70

Figure SI4.2D PDSD spectra of the T3SS needle. (A) Labeled with [1,3-^{13}C]glycerol, recorded on a 20.0 Tesla spectrometer (mixing time: 850ms). (B) Labeled with [2-^{13}C]glycerol, recorded on a 20.0 Tesla spectrometer (mixing time: 800ms). (C) Labeled with [2-^{13}C]glycerol, recorded on a 14.1 Tesla spectrometer (mixing time: 850ms).

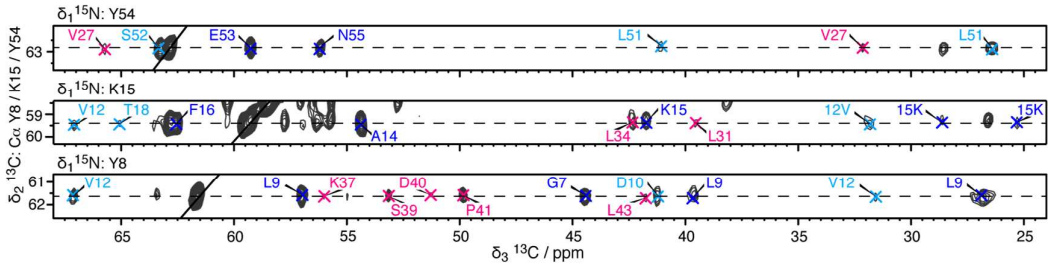

Figure SI5. Excerpts of the 3D ^{15}N-^{13}Cα-^{13}CX spectrum of the T3SS needle, labeled with [2-^{13}C]glycerol. Intra/sequential, medium-range (1<|i-j|<5) and long-range (|i-j|>4) restraints are colored in blue, cyan and pink, respectively.

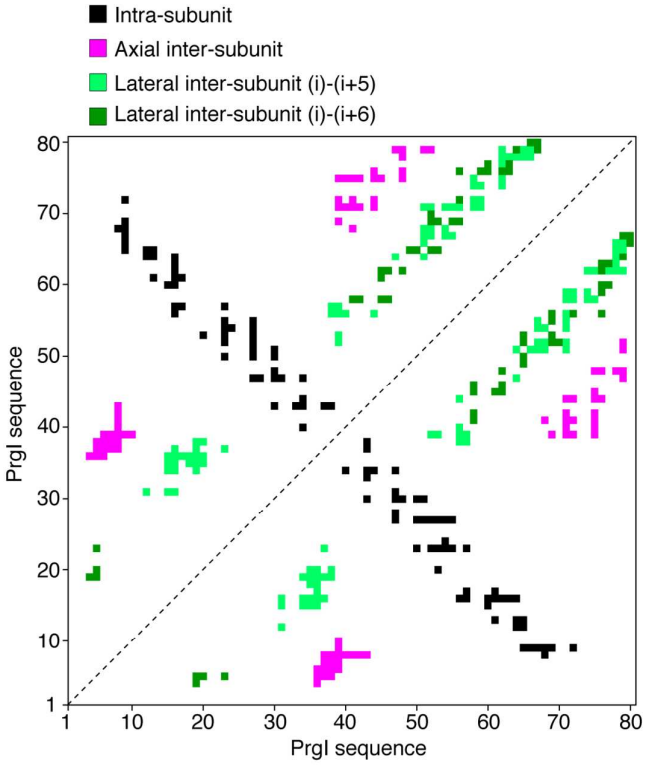

Figure SI6. Residue plot of the long-range distance restraints used for the structure calculation reported in this communication.

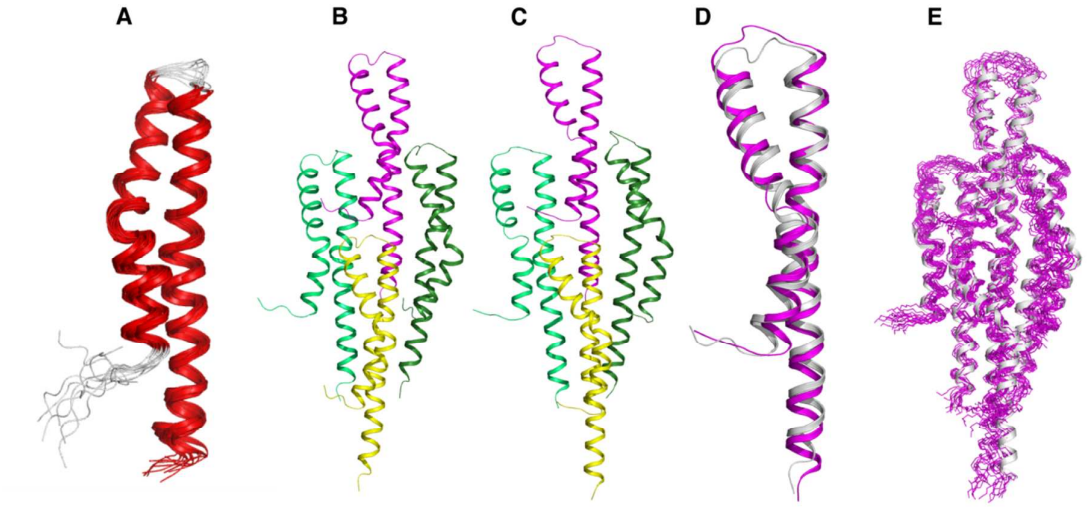

Figure SI7.(A) PrgI monomer (10 lowest-energy conformers). (B-C) Comparison of the tetrameric T3SS needle building block between the structure reported in (B) Loquet et al. (ref. 1) resulting from Rosetta modeling, (C) the present communication. (D) Overlay of monomeric PrgI between the Rosetta model (in grey) and the present study (in magenta). The backbone RMSD is 1.8Å. (E) Overlay of tetramericPrgI between the Rosetta model (cartoon representation, in grey) and the present study (in magenta). The backbone RMSD is 3.43Å.

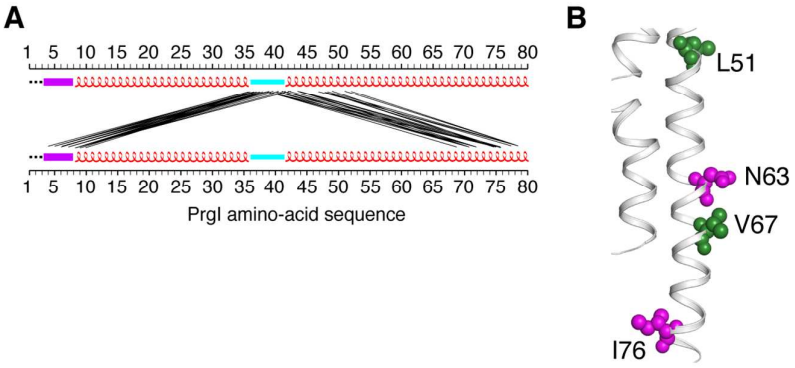

Figure SI8. (A) PrgI structure topology, plotted with axial inter-subunit restraints. These restraints, considering the helical topology, would lead as intra-subunit restraints to abnormal distortion of the helices and could therefore be unambiguously assigned to inter-subunit restraints. (B) Similarly, lateral restraints (here illustrated for residue pairs N63-I76 in magenta and L51-V67 in green) would lead to significant distortion if considered as intra-subunit restraints.

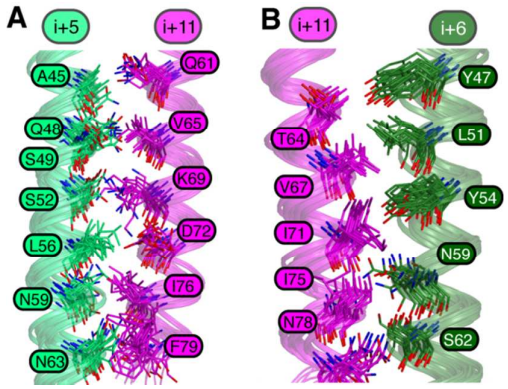

Figure SI9. Lateral supramolecular interfacesas determined by solid-state NMR, between (A) the T3SS needle subunits (i+5) and (i+11) and (B) the T3SS needle subunits (i+6) and (i+11).

Table SI1: SSNMR structure statistics.

Structural analysis	
Number of residues[a]	320 (4×80)
Number of models	15
Distance restraints[b] per asymmetric unit (tetramer)	
Total	1584 (1004 + 580)
Intra-subunit restraints (all)	1004 (4×251)
Inter-subunit restraints (all)	580
Inter-subunit restraints (axial interface)	208
Inter-subunit restraints (lateral interface (i/i+5))	212
Inter-subunit restraints (lateral interface (i/i+6))	160
Dihedral restraints (all)	624 (4×156)
R.m.s.d[c]	
Monomer(backbone atoms)	1.10Å ± 0.28 Å
Monomer (heavy atoms)	1. 62Å ± 0.24 Å
Tetramer (backbone atoms)	2.36Å± 0.72 Å
Tetramer (heavy atoms)	2.67 Å ± 0.67 Å
Violations	
Dihedral angle restraint violations(>5°)	0
Intra-subunit restraint violations (>1.5Å)	0
Intra-subunit restraint violations (>1.0Å)	1.27 ± 0.89
R.m.s.d. on intra-subunit restraints	0.19 ± 0.013
Inter-subunit restraint violations (>1.5Å)	0
Inter-subunit restraint violations (>1.0Å)	0.53 ± 0.743
R.m.s.d. on inter-subunit restraints	0.056 ± 0.016
Deviations from Idealized Covalent Geometry	
Bonds (Å)	0.0027 ± 0.0009
Angles (deg)	0.49 ± 0.027
Impropers (deg)	0.40 ± 0.016
Ramachandran Map Analysis[d]	
Most favorable regions	96.6%
Additionally allowed regions	3.4%
Generously allowed regions	0.0%
Disallowed regions	0.0%
Quality score[e]	
Procheck G-factor (phi / psi)	0.38
Verify3D	0.14 ± 0.018
ProsaII	0.36± 0.040

[a]Number of residues for the tetramer complex
[b]Only including long-range distances ($|i-j|>4$).
[c]Analysis of the structured core (P4-T18; L23-A36; A42-F79)
[d] Performed using PROCHECK-NMR[13]
[e]Performed using PSVS[14]

References

(1) Loquet, A.; Sgourakis, N. G.; Gupta, R.; Giller, K.; Riedel, D.; Goosmann, C.; Griesinger, C.; Kolbe, M.; Baker, D.; Becker, S.; Lange, A. *Nature***2012**, *486*, 276.
(2) Fung, B. M.; Khitrin, A. K.; Ermolaev, K. *J. Magn. Reson.***2000**, *142*, 97.
(3) Baldus, M.; Petkova, A. T.; Herzfeld, J.; Griffin, R. G. *Mol. Phys.***1998**, *95*, 1197.

(4) Castellani, F.; van Rossum, B. J.; Diehl, A.; Rehbein, K.; Oschkinat, H. *Biochemistry* **2003**, *42*, 11476.
(5) Habenstein, B.; Loquet, A.; Giller, K.; Becker, S.; Lange, A. *J Biomol NMR* **2013**, *55*, 1.
(6) Vranken, W. F.; Boucher, W.; Stevens, T. J.; Fogh, R. H.; Pajon, A.; Llinas, M.; Ulrich, E. L.; Markley, J. L.; Ionides, J.; Laue, E. D. *Proteins* **2005**, *59*, 687.
(7) Brunger, A. T. *Nat Protoc* **2007**, *2*, 2728.
(8) Shen, Y.; Delaglio, F.; Cornilescu, G.; Bax, A. *Journal of Biomolecular Nmr***2009**, *44*, 213.
(9) Bardiaux, B.; Malliavin, T.; Nilges, M. *Methods Mol Biol* **2012**, *831*, 453.
(10) Guerry, P.; Herrmann, T. *Methods Mol Biol* **2012**, *831*, 429.
(11) Wall, J. S.; Hainfeld, J. F. *Annu Rev Biophys Biophys Chem* **1986**, *15*, 355.
(12) Galkin, V. E.; Schmied, W. H.; Schraidt, O.; Marlovits, T. C.; Egelman, E. H. *J. Mol. Biol.* **2010**, *396*, 1392.
(13) Laskowski, R. A.; Rullmannn, J. A.; MacArthur, M. W.; Kaptein, R.; Thornton, J. M. *J Biomol NMR* **1996**, *8*, 477.
(14) Bhattacharya, A.; Tejero, R.; Montelione, G. T. *Proteins* **2007**, *66*, 778.